Cellular Signalling 125 (2025) 111494

Contents lists available at ScienceDirect

Cellular Signalling

journal homepage: www.elsevier.com/locate/cellsig

eIF3d specialized translation requires a RACK1-driven eIF3d binding to 43S PIC in proliferating SH-SY5Y neuroblastoma cells

Federica Silvestri [a], Raffaele Montuoro [b], Elisabetta Catalani [a], Francesca Tilesi [c], Daniela Willems [c], Nicla Romano [c], Sara Ricciardi [d,e], Davide Cervia [a], Marcello Ceci [c,*]

[a] Department for Innovation in Biological, Agro-food and Forest systems (DIBAF), Università degli Studi della Tuscia, Viterbo, Italy
[b] Department of Otolaryngology Head and Neck Surgery, Università Cattolica del Sacro Cuore, 00168 Rome, Italy
[c] Department of Ecological and Biological Science (DEB), Università degli Studi Della Tuscia, Viterbo, Italy
[d] National Institute of Molecular Genetics, INGM "Romeo ed Enrica Invernizzi", 20122 Milan, Italy
[e] Department of Biological Sciences, DBS, University of Milan, 20133 Milan, Italy

ARTICLE INFO

Keywords:
Translational control
eIF3d
RACK1
mTORC1
eIF4E
HSP-70

ABSTRACT

Translation initiation of most mammalian mRNAs is mediated by a 5′ cap structure that binds eukaryotic initiation factor 4E (eIF4E). Notably, most mRNAs are still capped when eIF4E is inhibited, suggesting alternative mechanisms likely mediate cap-dependent mRNA translation without functional eIF4F. Here we found that, when eIF4E is inhibited, the ribosomal scaffold RACK1 recruits eIF3d on the 43S pre-initiation complex. Moreover, we found that it is just PKCBII in its active form that promotes the binding of RACK1 to eIF3d. These studies disclose a previously unknown role of ribosomal RACK1 for eIF3d specialized translation.

1. Introduction

Translation of mRNAs into proteins is the most energy-consuming process in the cell and, therefore, is finely regulated by several mechanisms [1]. Regulation is mostly exerted at the initiation step, which is generally considered the rate-limiting step in protein synthesis [2]. In eukaryotes, the canonical cap-dependent translation initiation is a complicated process that depends on the cooperation of many translation initiation factors (eIFs) [3]. These cooperate in (i) recognizing the 5′-end of the mRNA by binding to its 5′-cap structure, (ii) recruiting the 40S ribosomal subunit to the 5′-end, (iii) scanning of the 43S pre-initiation complex (PIC) along the 5′-untranslated region (5′-UTR) to the AUG start codon and, (iv) joining the large (60S) ribosomal subunit to form a functional ribosome [4].

Specifically, the eukaryotic initiation factors eIF1, eIF1A, eIF3, and eIF5 and the ternary complex (TC) of eIF2–guanosine 5′-triphosphate (GTP)–methionine initiator transfer RNA (tRNAiMet) first binds to the 40S ribosomal subunit to form the 43S PIC [5]. Once assembled, the 43S PIC is recruited to the cap-binding complex eIF4F at the 5′ end of mRNA to form a 48S initiation complex. This scans the mRNA in the 5′–3′ direction until a start codon is found [3].

eIF4F is a heterotrimeric complex composed of eIF4E, the DEAD-box helicase eIF4A and eIF4G. eIF4E binds the 7-methylguanosine (7-m-GTP) cap, whereas eIF4A unwinds the secondary structures in the 5′ untranslated regions (UTR) of the mRNAs [6]. The scaffold protein eIF4G, besides recruiting the 43S PIC through the interaction with eIF3, promotes the circularization of mRNAs by interacting with the poly-A binding proteins (PABPs) [7].

The eIF4E component of the eIF4F complex is generally considered to be the rate-limiting factor in translation initiation and, therefore, its availability is tightly controlled through a regulated interaction with eIF4E-binding proteins (4E-BPs) [8]. These proteins function as competitive inhibitors of the binding of eIF4E to eIF4G resulting in the inhibition of the eIF4F complex from initiating mRNA translation. Instead, the mammalian target of rapamycin (mTOR) plays an essential role in promoting mRNA translation by directly phosphorylating and inhibiting 4E-BPs [9]. Actually, under normal growth conditions, activated mTORC1 phosphorylates eIF4E-binding proteins (4E-BPs) resulting in the release of eIF4E from 4E-BPs and leading to an increase in the translation of a pool of mRNAs often referred to as "eIF4E-sensitive" [10].

A multitude of stresses inhibit mTORC1 activity resulting in

* Corresponding author.
E-mail addresses: federica.silvestri@unitus.it (F. Silvestri), ecatalani@unitus.it (E. Catalani), francesca.tilesi@unitus.it (F. Tilesi), willems@unitus.it (D. Willems), nromano@unitus.it (N. Romano), ricciardi@unimi.it (S. Ricciardi), d.cervia@unitus.it (D. Cervia), m.ceci@unitus.it (M. Ceci).

https://doi.org/10.1016/j.cellsig.2024.111494
Received 25 March 2024; Received in revised form 19 October 2024; Accepted 27 October 2024
Available online 29 October 2024

hypophosphorylated 4E-BPs that sequester eIF4E [11]. However, upon mTORC1 inhibition, the overall translation is reduced by only 60 %. This does not necessarily mean that the remaining 40 % of translation solely relies on cap-independent mechanisms [12]. Notably, most mRNAs are still capped when the canonical eIF4F is inhibited, suggesting that alternative mechanisms likely exist to mediate cap-dependent mRNA translation in the absence of functional eIF4F [2].

EIF3d, one of the eIF3 subunits, which is the largest and most complex initiation factor that binds to the solvent-exposed side of the 40S ribosome, has been recognized as another mRNA cap-binding protein [13]. eIF3d has been reported to interact directly with the 5′-cap mRNAs, indicating that eIF3d may help recruit mRNAs to the 43S PICs independent of eIF4F [14]. Thus, there may be an alternate or noncanonical cap-dependent initiation mechanism via eIF3d, different from the canonical cap-dependent translation initiation via eIF4F [15]. It is just by interacting with DAP5, a member of the eIF4G family, that eIF3d contributes to the translation of approximately 20 % of mRNAs when the eIF4F-dependent translation is inhibited [16]. The noncanonical regulation of mRNA translation may contribute to the role of eIF3d in biological processes such as metabolic stress adaptation, chronic glucose deprivation, disease onset and progression, including tumorigenesis and acquired immune deficiency syndrome [17].

The mammalian eIF3 complex has a molecular weight of 800 kDa and is composed of 13 subunits (eIF3a through eIF3m) organized in two major modules [18], the Proteasome COP9-signalosome eIF3/Mpr1, Pad1_N-terminal (PCI/MPN) octamer core and five peripheral subunits flexibly linked to the octamer core. Recent structural studies have detailed the architecture of mammalian and yeast eIF3 complexes in the context of the 43S PIC [19–22] and 48S PICs [23]. Interestingly, these studies proved that the peripheral subunit, eIF3d, is located on the opposite site of the mRNA channel, near the exit and adjacent to the ribosomal protein that is the receptor for the activated C kinase 1 (RACK1) [19].

This finding is intriguing since RACK1 is not only a core component of the ribosomal 40S subunit but is by itself a regulator of global and specific translations in different ways [24]. RACK1 functions as a molecular ship that shuttles the activated protein kinase C βII (PKCβII) [25], but it may also interact with various other signaling proteins, including integrin and Src protein-tyrosine kinase [26–29]. The interaction between RACK1 and various proteins in different cellular compartments makes RACK1 relevant in many physiological processes, such as cell motility, cell survival and death, proliferation, immune signaling, tumorigenesis, and neuronal function [30–33]. Thus, eIF3d and RACK1 may coordinate in the noncanonical cap-independent translation initiation. Information on this novel mechanism of cap-independent translation initiation still lacking, however. Herein, we show that RACK1 recruits eIF3d on 43S PIC for the synthesis of the HSP-70 protein and that this occurs during heat stress and when eIF4F is inhibited. Furthermore, we demonstrate that the active PKCβII kinase promotes the binding of eIF3d with ribosomal RACK1.

2. Materials and methods

2.1. Cell culture and treatments

Neuroblastoma SH-SY5Y, MCF-7 and MDA-MB-231 cell lines were purchased from the ATCC (American Type Culture Collection) and maintained at 37 °C under 5 % CO_2 in Dulbecco's Modified Eagle Medium: Nutrient Mixture F12 (DMEM F12) supplemented with 10 % fetal bovine serum (FBS) and antibiotics.

Cells stably expressing R36D K38E mutant or wild-type RACK1, both fused to histidine-my tag ($RACK1_{DE\text{-}his\text{-}myc}$ or $RACK1_{WThis\text{-}myc}$) were produced as in [34]. For eIF3d transient over-expression, SH-SY5Y cells were transfected with Lipofecatimine 2000 (ThermoFisher), following the manufacturer's instructions. The pcDNA5/FRT eIF3d-HA plasmid was gently provided by Cate Lab. For PKCβII transient expression, cells stably expressing $RACK1_{WT\text{-}his\text{-}myc}$ were transfected by Lipofectamine 2000 (ThermoFisher), following the manufacturer's instructions, with pcDNA3-GFP PKCβII constitutively active, termed C.A., or the pcDNA3-GFP PKCβII kinase-dead, termed K.D., encoding for a mutated form of PKCβII, gently provided by prof. Alexandra Newton (University of California at San Diego) [35]. A list of the cell lines used for the experiments is reported below:

Cell line	Genotype	Identifier
SH-SH5Y	Empty plasmid	CTRL
SH-SH5Y	$RACK1_{WT\text{-}his\text{-}myc}$	WT
SH-SH5Y	$RACK1_{DE\text{-}his\text{-}myc}$	DE
SH-SH5Y	$eIF3d_{HA}$	$eIF3d_{HA}$
SH-SH5Y	$RACK1_{WT\text{-}his\text{-}myc}/eIF3d_{HA}$	$WT/eIF3d_{HA}$
SH-SH5Y	$RACK1_{DE\text{-}his\text{-}myc}/eIF3d_{HA}$	$DE/eIF3d_{HA}$
SH-SH5Y	$RACK1_{WT\text{-}his\text{-}myc}$/GFP-PKCβII C.A.	WT/C.A.
SH-SH5Y	$RACK1_{WT\text{-}his\text{-}myc}$/GFP-PKCβII K.D.	WT/K.D.
MCF-7	$RACK1_{WT\text{-}his\text{-}myc}$	WT
MDA-MB-231	$RACK1_{WT\text{-}his\text{-}myc}$	WT

Where indicated, cells were serum-starved and then treated with Rapamycin 500 nM (Sigma-Aldrich) for 1 h. For heat exposure, 44 °C was applied for 30 min without serum starvation [36].

2.2. Polysomal profiles

Polysomal profiles were performed as previously described [37]. Briefly, cells were lysed in 10 mM Tris-HCl, 50 mM KCl, 10 mM $MgCl_2$ and 0.5 % NP-40. Lysates were clarified at 14,000 r.p.m. for 5 min at 4 °C and cytoplasmic extracts were loaded on a 15–50 % sucrose gradient and centrifuged at 4 °C in a SW41Ti Beckman rotor for 2 h at 37,000 r.p.m. Absorbance at 254 nm was recorded by BioLogic LP software (BioRad) and fractions (1 ml each) were collected for subsequent protein extraction.

Proteins from individual polysome fractions were isolated using TCA/Deoxycholate precipitation. Briefly, deoxycholate was added to each fraction at a final concentration of 0.01 % (*v*/v) and incubated on ice for 30 min. Next, 100 % TCA was added to each fraction (final TCA concentration is 10 % (v/v) and incubated on ice for a further 30 min. The mixture was then centrifuged at 14,000 *g* at 4 °C for 30 min. The supernatant was carefully discarded, and the pellet was washed with 1 volume of ice-cold acetone, centrifuged at 14,000 *g* at 4 °C for 10 min and resulting pellets were allowed to air dry for ~10 min in a fume hood. Individual fractions were re-suspended in 2× Laemmli Sample Buffer (125 mM Tris-HCl, pH 68, 20 % Glycerol, 10 % SDS 10 %, 1 M DTT, 0,004 % Bromophenol blue) with 2-mercaptoethanol and equal volumes of fractions were subjected to western blot analysis.

2.3. Histidine protein interaction pull-down (HPIPD)

Histidine pull-down was performed as previously described [34]. Briefly, after 2 washes in PBS 1× (Na2HPO4 8 mM, KHPO4 1,4 mM, NaCl 140 mM, KCl 1,7 mM), cells were lysed in 10 mM Tris-HCl, 50 mM KCl, 10 mM $MgCl_2$ and 0,5 % NP-40 and centrifugated at 14,000 r.p.m. for 5 min at 4 °C. Cell lysates were then incubated with the indicated nickel affinity resin (Biorad) for 2 h. Immunoprecipitates were subsequently washed three times in lysis buffer using purification columns (Biorad), and eluted using 10 mM Tris-HCl, 50 mM KCl, 10 mM $MgCl_2$ and 0,5 % NP-40 containing 300 mM Imidazole. Eluted proteins were isolated using the previously described TCA/Deoxycholate precipitation and subjected to western blot analysis. For histidine pull down in presence of RNase I, protein extracts, were or not treated with 50 μg/ml of RNase I for 30 min at room temperature before histidine purification as previously seen. [36]

2.4. Cap-binding assays

For cap-binding assays, cells were lysed in 10 mM Tris-HCl, 50 mM KCl, 10 mM $MgCl_2$ and 0,5 % NP-40. Cell lysates were incubated with 7-methyl-GTP Sepharose (GE Healthcare) for 2 h and then clarified at 14,000 r.p.m. for 15 min at 4 °C. Pull-downs were eluted with 1× Laemmli Sample Buffer and then subjected to immunoblotting as described later.

2.5. SUnSET assay

The rate of protein synthesis was measured using the SUnSET assay as reported in [34]. Briefly, cells were treated with 5 μg/ml puromycin for 10 min at 37 °C under 5 % CO_2. Following treatment, cells were lysed in 10 mM Tris-HCl, 50 mM KCl, 10 mM $MgCl_2$ and 0,5 % NP-40. Lysates were then clarified at 14,000 r.p.m. for 5 min at 4 °C. Puromycin incorporation was then determined by Western blotting, as described later.

2.6. SDS-PAGE and Western blotting

SDS-PAGE and Western blotting were performed on protein extracts obtained from cells lysed in 10 mM Tris-HCl, pH 7.6, 100 mM NaCl, 100 mM MgCl, Triton 0.1 % supplemented with complete Protease Inhibitor Cocktail (ROCHE). Cell lysates were separated by SDS-PAGE and transferred to polyvinylidene fluoride membranes (Millipore). Immunoblotting was performed using the following primary antibodies:

antibody	Source	Identifier
β-Actin	Cell Signaling	4967
eIF3d	Proteintech	10,219
eIF4E	Cell Signaling	9742
eIF4G	Cell Signaling	2498
GFP	Abcam	13,970
HA	Cell Signaling	C29F4
HSP70	Sigma-Aldrich	H5147
Myc-tag (9B11)	Cell Signaling	2276
Puromycin	Merck-Millipore	MABE343
RACK1	BD Transduction Laboratories™	610,178
PKCβII	BD Transduction Laboratories™	610,127
Ribosomal Protein S6	Cell Signaling	4858
Cyclin D2	Cell Signaling	3741

Subsequently, membranes were incubated with secondary anti-IgM (Sigma Aldrich) or anti-IgG mouse or rabbit HRP-tagged antibodies (GE Healthcare, 1:5000; Sigma, 1:5000) and the chemiluminescent signals were detected with Amersham ECL Prime (Thermo Fisher Scientific) using the iBrightTM CL750 Imaging System (Thermo Fisher Scientific).

2.7. RNA extraction and quantitative RT-PCR

Total RNA was purified with TRIzol reagent (ThermoFisher) from SH-SY5Y cells stably expressing $RACK1_{DE\text{-}his\text{-}myc}$ or $RACK1_{WThis\text{-}myc}$ and transfected with cDNA5/FRT eIF3d-HA plasmid.

Gene expression analysis was performed by quantitative real-time RT-PCR (qPCR) using SYBR Green PCR Master Mix (Promega) with the following pairs of primers: HSP-70 forward, 5'-AGGCCGACAAGAAGAAGGTGCT-3′, HSP-70 reverse, 5'-TGGTACAGTCCGCTGATGATGG-3′; Cyclin D2 forward primer- 5'-GCAAATGTGTACGTGCATGC-3′, reverse 5'-CGATGATTTGCTGGGGATG-3 GAPDH forward 5'-GAAGGTGAAGGTCGGAGTC-3′, GAPDH reverse 5'-CCCGAATCACATTCTCCAAGAA-3′.

2.8. Statistical analysis

The statistical significance of raw data between the groups one-way ANOVA followed by the Tukey post-test (multiple comparisons). A *p*-value ≤0.05 is considered statistically significant. * < 0,05, ** < 0,01, *** < 0,001 **** < 0,0001. The GraphPad Prism software package (GraphPad Software, San Diego, CA, USA) was used. The results were expressed as means ± s.d.

3. Results

3.1. RACK1 recruits eIF3d on the translational machinery

To identify the translational signaling pathway used by the ribosomal RACK1 to increase the SH-SY5Y cell cycle [34], we looked at its position on the 40S ribosomal subunit. The 43/48S PIC cryo-EM elaborations show that ribosomal RACK1 lies in the exit mRNA channel between two subunits of the eIF3 multi-complex, the eIF3a and eIF3d proteins [19], which are both involved in cell proliferation [19,38,39]. Of the two proteins, the interaction of RACK1 with eIF3a excludes a possible role in cell proliferation [40,41], while its interaction with eIF3d is not examined yet. Therefore, we wondered whether the eIF3d impacts the ribosomal RACK1 activity to raise the cell cycle. To this end, we initially compared the ribosomal distribution of eIF3d on the translational machinery between down-proliferating SH-SY5Y cells expressing the ribosomal-low affinity RACK1 mutant (R36D/K38E, $RACK1_{DE\text{-}his\text{-}myc}$) and over-proliferating cells expressing the wild-type RACK1 ($RACK1_{WT\text{-}his\text{-}myc}$) [42]. The ribosomal RACK1 mutant expression in yeast and mammalian cells reduces the binding of RNA-binding proteins, such as α-Scp160, TDP-43, and FMRP, and kinases such as the PKCβII to translational machinery [33,36,42,43]. Moreover, its expression induces cellular defects likely to those caused by the RACK1 depletion in both yeast and neurons [33,44]. For this, the RACK1 mutant may be useful to investigate the role of eIF3d in the ribosomal RACK1 function. As previously reported [34], in the over-proliferating cells, $RACK1_{WT}$ was mainly present on the 40S and 80S ribosomes while the endogenous RACK1 was equally distributed on monosomes (40S, 60S free ribosomes and 80S) and polyribosomes (Fig. 1A and Supplemental Fig. 1A). In contrast, in down-proliferating cells, the mutant RACK1 accumulates at the top gradient, out from monosomes and polyribosomes without affecting the ribosomal distribution of endogenous RACK1 (Fig. 1B and Supplemental Fig. 1A). The eIF3d immunoblotting found that eIF3d *co*-sedimented with $RACK1_{WT\text{-}his\text{-}myc}$ and endogenous RACK1 on free monosomes and polyribosomes in the $RACK1_{WT\text{-}his\text{-}myc}$ cells. Instead, in the $RACK1_{DE\text{-}his\text{-}myc}$ cells, eIF3d behaved as mutant RACK1. It accumulated at the top of the gradient, excluded from ribosomal fractions (Fig. 1A, B and C). To confirm the abnormal ribosomal distribution of eIF3d depended on the RACK1 mutant expression, we examined whether the eIF4E distribution, which is distant from eIF3d and RACK1 on the 40S subunit (picture in Fig. 1E) [19], was also affected. The eIF4E immunoblotting revealed that the eIF4E was equally distributed in the $RACK1_{DE\text{-}his\text{-}myc}$ and $RACK1_{WT\text{-}his\text{-}myc}$ polysomal profiles (Fig. 1A, B and C), and thus its ribosomal distribution was unaffected by the $RACK1_{DE\text{-}his\text{-}myc}$ expression. To exclude that free ribosomes and polyribosomes were differently purified, we examined the levels of rps6 in the collected fractions. Free ribosomes and polyribosomes revealed similar levels of rps6 by immunoblotting demonstrating the translational machinery was equally purified by $RACK1_{DE\text{-}his\text{-}myc}$ and $RACK1_{WT\text{-}his\text{-}myc}$ polysomal profiles.

To further examine whether the $RACK1_{DE\text{-}his\text{-}myc}$ expression modifies the association of eIF3d with translational machinery, we examined its m^7GTP cap affinity by m^7GTP cap-binding chromatography [15]. The eIF3d resulted in being weakly cap-purified in the case of control cells transfected with empty plasmid and in mutant RACK1 cells, but more significantly purified in the case of cells expressing $RACK1_{WT\text{-}his\text{-}myc}$ (Fig. 1D and bar graph). As observed in polysomal fractions, the expression of the RACK1 mutant unaffected the level of the endogenous RACK1 purified with the cap chromatography (Fig. 1D), implying that the RACK1 mutant expression alters the binding of eIF3d to translational apparatus in down-proliferating cells.

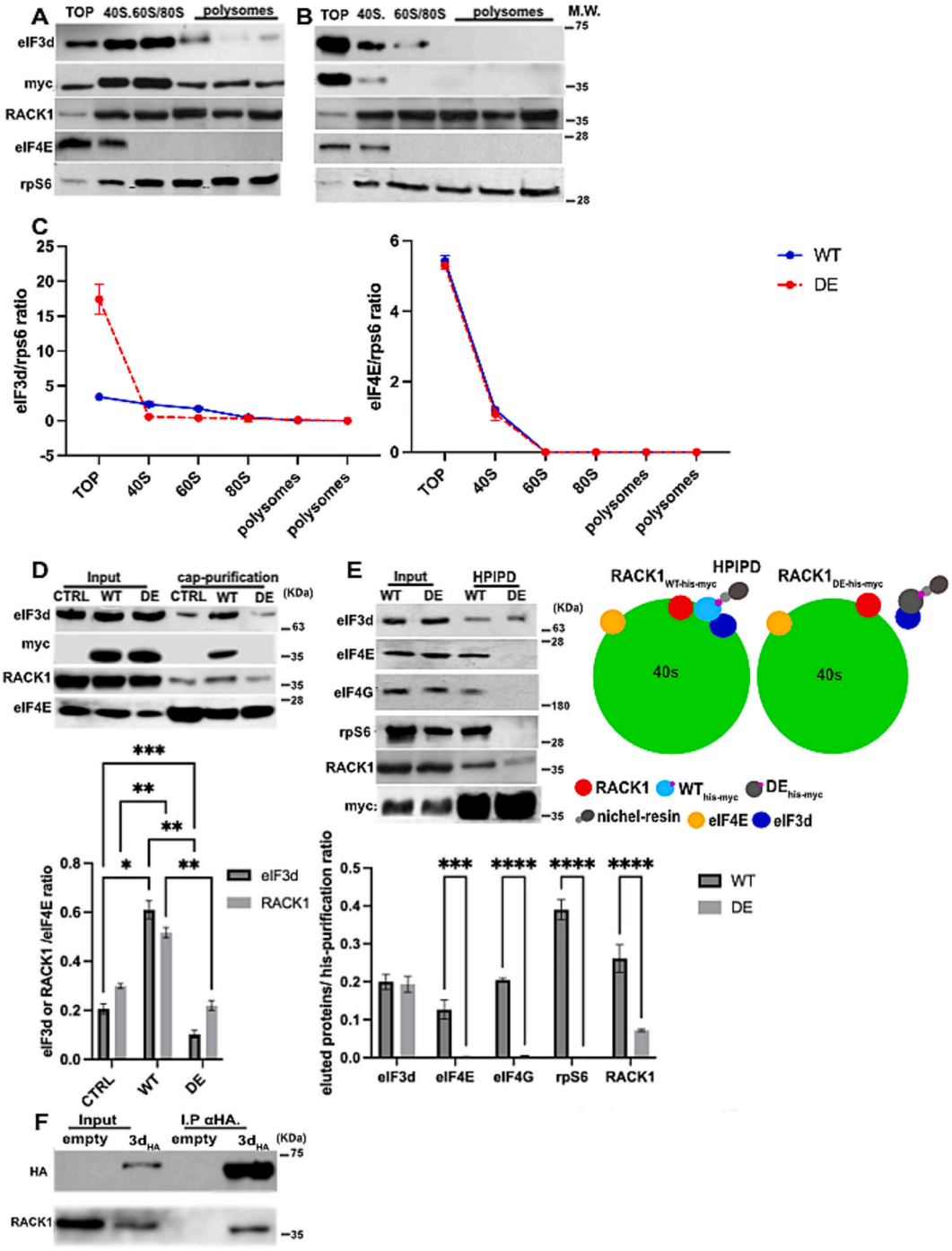

Fig. 1. Ribosomal RACK1 recruits eIF3d on the translational machinery. A) and B) Representative immunoblotting ($n = 3$ independent experiments) showing the expression of eIF3d, myc, eIF4E, RACK1 and Rps6 on collected polysomal fractions of SHSY5Y human neuroblastoma cells stably expressing $RACK1_{WT\text{-}his\text{-}myc}$ A) or and $RACK1_{DE\text{-}his\text{-}myc}$ B). C) Quantifying eIF3d levels normalized to Rps6 level on polysomal fractions of $RACK1_{WT\text{-}his\text{-}myc}$ and $RACK1_{DE\text{-}his\text{-}myc}$ SHSY5Y cells. Data reported as mean ± sd. D) Representative immunoblotting (n = 3 independent experiments) showing the expression of eIF3d, eIF4E, RACK1 and myc on both total lysate and m^7GTP eluate in control (CTRL), $RACK1_{DE\text{-}}$ (DE) and $RACK1_{WT\text{-}his\text{-}myc}$ (WT) cells. The bar graph (*lower*) reports the band intensity ratio between eIF3d, RACK1 and myc to eIF4E on the eluted proteins (Arbitrary units). Data are mean ± sd. E) Representative immunoblotting ($n = 3$ independent experiments) showing the expression of eIF3d, eIF4E, eIF4G, RACK1, Rps6 and myc on both, total lysate and His pull-down eluate in $RACK1_{DE\text{-}}$ (DE) and $RACK1_{WT\text{-}his\text{-}myc}$ (WT) cells. The bar graph (*lower*) reports the band intensity ratio between eIF3d, eIF4E, eIF4G, RACK1, and Rps6 to Myc. Data are mean ± sd. The picture shows endogenous RACK1, eIF3d and eIF4E associated with 40S ribosomal protein in control cells (SH-SY5Y), $RACK1_{DE\text{-}his\text{-}myc\ and}$ $RACK1_{WT\text{-}his\text{-}myc,}$ eIF3d and eIF4E associated with 40S ribosomal protein in $RACK1_{WT\text{-}his\text{-}myc}$ and $RACK1_{WT\text{-}his\text{-}myc}$ cells, respectively. Moreover, the picture shows the nickel-resin affinity in His purification. F) Representative immunoblotting (n = 3 independent experiments) showing the expression of RACK1 and $eIF3d_{HA}$ on immunoprecipitation eluate in SH-SY5Y cells expressing either $eIF3d_{HA}$ ($3d_{HA}$) or empty plasmid (control).

To understand how the expression of the RACK1 mutant modifies the ribosomal affinity of eIF3d, we thought that the RACK1 mutant and eIF3d form a complex from which eIF4E and ribosomes are excluded. For this, a co-purification assay by a Histidine pull down from $RACK1_{DE\text{-}his\text{-}myc}$ and $RACK1_{WT\text{-}his\text{-}myc}$ cells (picture Fig. 1E) studied the binding of eIF3d, eIF4E and rps6 with them by immunoblotting on imidazole eluted proteins. The assay proved that eIF3d co-purified with $RACK1_{DE\text{-}his\text{-}myc}$ and $RACK1_{WT\text{-}his\text{-}myc}$ similarly, while rpS6, eIF4E and eIF4G co-purified with $RACK1_{WT\text{-}his\text{-}myc}$ but not with mutant RACK1 (Fig. 1E and bar graph). Worth noting, the presence of eIF3d, eIF4E, eIF4G and RpS6 proteins in $RACK1_{WT\text{-}his\text{-}myc}$ his protein interaction pull-down (HPIPD) assay implies that the 43S/48S complexes (PICs) are also purified with $RACK1_{WT\text{-}his\text{-}myc}$ protein. In turn, this suggested that $RACK1_{WT\text{-}his\text{-}myc}$ HPIPD is a useful tool for PIC isolation. Thus, the binding of eIF3d with the $RACK1_{DE\text{-}his\text{-}myc}$ explains the decline of the eIF3d on translational machinery, most likely to PICs, and demonstrates that ribosomal RACK1 is required to recruit eIF3d to PICs. Interestingly, although the endogenous RACK1 expression was unaffected by the mutant and wild-type RACK1 expression, a small amount of endogenous RACK1 copurified with the RACK1 mutant (Fig. 1E, bar graph and Supplemental Fig. 1B), suggesting that a no-significant amount of endogenous RACK1 may be removed by PICs.

To further support that RACK1 binds eIF3d we performed a reciprocal co-purification assay. To this end, N-terminal eIF3d tagged with hemaglutinin ($eIF3d_{HA}$) was expressed in SH-SY5Y neuroblastoma cells, along with empty vector plasmid and its binding to the endogenous RACK1 was analyzed by HA-immunoprecipitation. Although the RACK1 expression was decreased by the $eIF3d_{HA}$ up-regulation, in agreement with the HPIPD results, RACK1 co-immunoprecipitates with $eIF3d_{HA}$ (Fig. 1F). In addition, we performed the HPIPD assay after RNAse treatment to verify whether the interaction between the $RACK1_{WT\text{-}his\text{-}myc}$ and eIF3d was RNA-dependent. We found that RNAse did not affect the binding of $RACK1_{WT\text{-}his\text{-}myc}$ to eIF3d (Supplemental Fig. 2) demonstrating that RACK1 and eIF3d form a biochemical complex independent of RNA.

3.2. *eIF3d-RACK1 binding contributes to the specific translation of cyclin D2 mRNA*

We were next interested in understanding whether the RACK1-mediated eIF3d recruitment on PICs induced the translation of specific mRNAs encoding for cell cycle proteins. To this end, we examined the translation of the cyclin D2 mRNA because it is among mRNAs binding to eIF3d [14] and is translationally regulated by $RACK1_{WT\text{-}his\text{-}myc}$ [34,43], representing an ideal target mRNA. To study whether the cyclin D2 mRNA translation is modulated by the binding of eIF3d to RACK1 on PICs, we analyzed its translation when the eIF3d is not associated or associated with PICs. To this aim, $eIF3d_{HA}$ has been expressed in $RACK1_{DE\text{-}his\text{-}myc}$ and $RACK1_{WT\text{-}his\text{-}myc}$ cells and its absence or presence on PICs has been analyzed by cap chromatography and HPIPD assay. $eIF3d_{HA}$ increased its cap affinity when $RACK1_{WT\text{-}his\text{-}myc}$ bound to the cap structure, while it was countered by the absence of the RACK1 mutant from the cap element (Fig. 2A). Interestingly, the affinity of eIF4E for cap-element decreased as the cap-binding of $eIF3d_{HA}$ increased (Fig. 2A and *bar graph lower*). In agreement with this, the HPIPD assay displayed that the binding of $eIF3d_{HA}$ with $RACK1_{WT\text{-}his\text{-}myc}$ excluded eIF4E from the His purification (Fig. 2B). Therefore, the $RACK1_{WT\text{-}his\text{-}myc}$ expression localizes the $eIF3d_{HA}$ on PICs and the RACK1 mutant excludes it from them. Under these conditions, the cyclin D2 expression shows the highest increase when $eIF3d_{HA}$ was expressed with $RACK1_{WT\text{-}his\text{-}myc}$ (Fig. 2C and bar graph), even more elevated than cells expressing $eIF3d_{HA}$ or the $RACK1_{WT\text{-}his\text{-}myc}$ that were already higher compared to control (Fig. 2C and bar graph), in agreement with previous reports [34,45,46]. In contrast, the expression of $eIF3d_{HA}$ in the $RACK1_{DE\text{-}his\text{-}myc}$ cells failed to increase the cyclin D2 expression maintaining to levels to the RACK1 mutant alone (Fig. 2C and bar graph), just as previously reported [34].

To exclude that the different translation of cyclin D2 mRNA was due to changes in the global translation, we analyzed the protein synthesis rate by the SUnSET assay. This showed that cells expressing $eIF3d_{HA}$ incorporate less puromycin than all other cases (Fig. 2C), suggesting that $eIF3d_{HA}$ decreases the translation rate. $RACK1_{WT\text{-}his\text{-}myc}$ fails to normalize the $eIF3d_{HA}$-induced translation decrease, while the RACK1 mutant expression restored the translation rate to the control levels (Fig. 2C).

To finally confirm that the cyclin D2 expression was translationally controlled by the eIF3d-RACK1 complex we measured its mRNA level by the qRT-PCR assay. The level of cyclin D2 mRNA was unaffected by the eIF3d, RACK1, or both upregulation (Fig. 2D).

Thus, the recruitment of eIF3 of PIC by ribosomal RACK1 induces the translation of cyclin D2 mRNA.

3.3. *The active form of PKCBII promotes the binding of RACK1 to eIF3d and the cyclin D2 expression*

Next, to understand which translationally controlling pathways might regulate the binding of RACK1 with eIF3d, we considered the function of anchoring to the translational machinery of ribosomal RACK1 for the active PKCβII in the phosphorylation of the eIF6 in 80S ribosomal joining and the phosphorylation of eIF4G [41,47,48]. To verify whether the active PKCβII also modulates the binding of RACK1 to eIF3d, we monitored the interaction of eIF3d with $RACK1_{WT\text{-}his\text{-}myc}$ by HPIPD assay when a GFP-tagged active (constitutively active, C.A.) or inactive (kinase-dead, K.D.) PKCβII [35] were expressed in the $RACK1_{WT\text{-}his\text{-}myc}$ SH-SY5Y cells. The eIF3d immunoblotting reveals that the active PKCβII increases the eIF3d binding to $RACK1_{WT\text{-}his\text{-}myc}$ compared to the control cells (transfected with the empty vector plasmid) (Fig. 3). Instead, the inactive PKCβII, as well as for the control case, does not modify this binding. This suggests that the RACK1-eIF3d complex is sensitive to active PKCβII. In support of this, the active PKCβII is co-purified with eIF3d and $RACK1_{WT\text{-}his\text{-}myc}$, in contrast to the inactive PKCβII, which is absent from the purification (Fig. 3). To further investigate whether the active PKCβII promotes the association of RACK1 with eIF3d, we induced the neuronal cell differentiation signal, which relies on the PKC beta activation [49,50] in the $RACK1_{WT\text{-}his\text{-}myc}$ SH-SY5Y cells, and led the HPIPD assay. Aphidicolin (0,3 μM) and NGF (100 ng/ml) administration, required for SH-SY5Y cell differentiation [51,52], increases the binding of ribosomal RACK1 to eIF3d (Supplemental Fig. 3), corroborating the positive effect of the active PKCβII on the ribosomal RACK1-eIF3d interaction.

To further understand whether the active PKCβII regulates the activity of the RACK1-eIF3d complex, we measured the expression of cyclin D2. In agreement with the active PKCβII results, the cyclin D2 expression increased in cells expressing active PKCβII more than in inactive PKCβII and control cells (Fig. 3). Thus, the active PKCBII stimulates the association of RACK1 with eIF3d and the expression of cyclin D2.

3.4. *The eIF4E canonical translation blocking induces the binding of RACK1 to eIF3d promoting the HSP-70 mRNA translation*

Accumulating evidence reveals that eIF3d specialized translation is critical during eIF4F blocking conditions [12,15,53]. Therefore, we wondered whether the binding of ribosomal RACK1 to eIF3d studied by the HPIPD assay might be modulated under the rapamycin administration or heat shock stress, two conditions inhibiting eIF4E canonical-dependent translation [54,55]. We found that both treatments increased the association of eIF3d with $RACK1_{WT\text{-}his\text{-}myc}$ (Fig. 4A), at the same time the level of the co-purification of eIF4E with $RACK1_{WT\text{-}his\text{-}myc}$ decreased, inhibiting the eIF4F complex, and the global translation rate was reduced (Fig. 4A and B). As RACK1 up-regulation also stimulates the proliferation rate of MCF-7 and MDA cells [34], we repeated the HPIPD

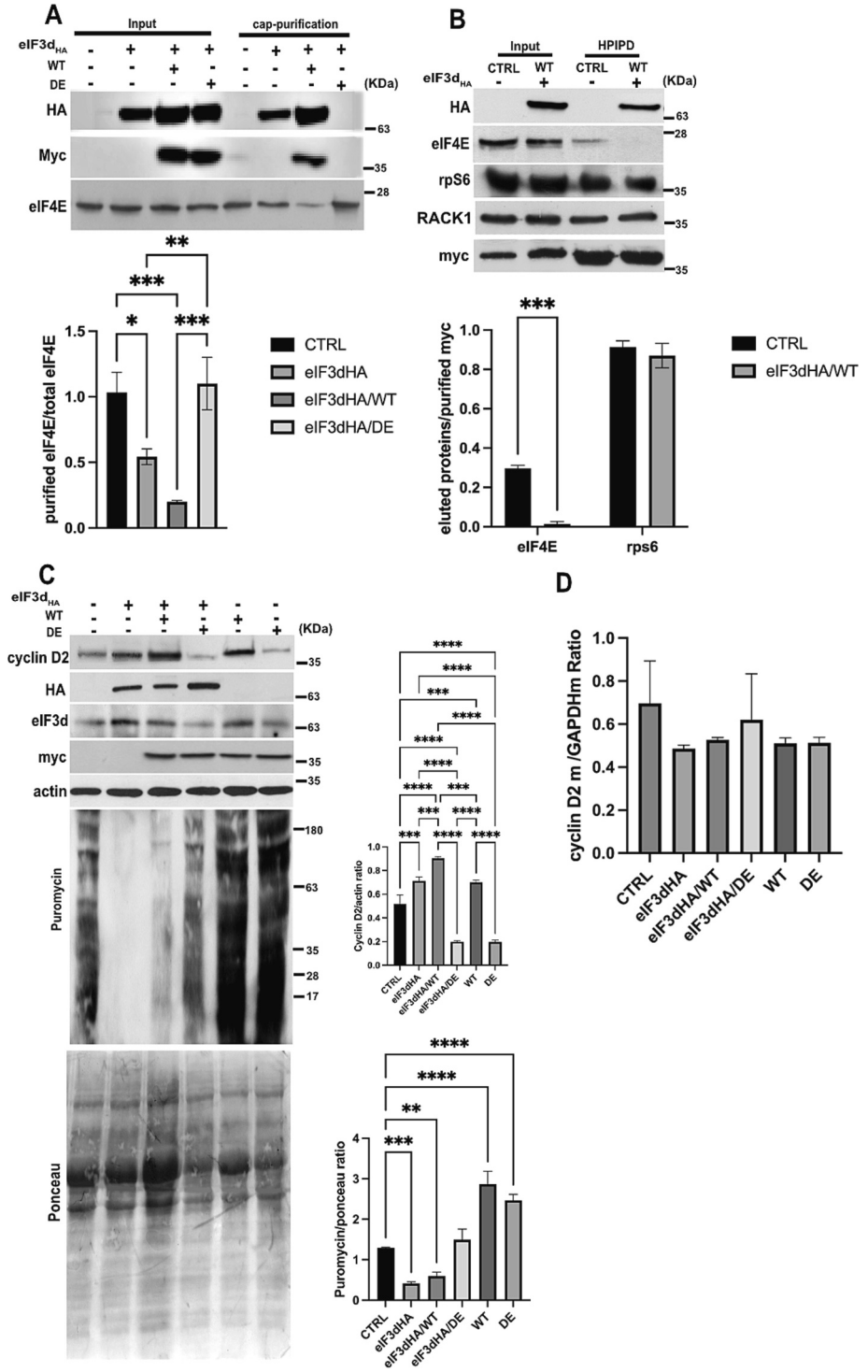

Fig. 2. The ribosomal RACK1/eIF3d complex regulates the cyclin D2 protein expression. A) Representative immunoblotting ($n = 3$ independent experiments) showing the expression of HA, myc and eIF4E on total lysate and m^7GTP eluate in control, $RACK1_{DE-}$ (DE) and $RACK1_{WT\text{-}his\text{-}myc}$ (WT) cells, expressing or not the $eIF3D_{HA}$ protein. The bar graph (*lower*) reports the ratio of band intensity between purified eIF4E to total eIF4E. Data are mean ± sd B) Representative immunoblotting (n = 3 independent experiments) shows the expression of HA, eIF4E, Rps6, RACK1 and myc on both, total lysate and His pull-down eluate in $RACK1_{WT\text{-}his\text{-}myc}$ (WT) expressing or not the $eIF3D_{HA}$ protein. The bar graph (*lower*) reports the ratio of band intensity between HA, eIF4E and Rps6 to Myc. Data are mean ± sd. C) Representative immunoblotting (n = 3 independent experiments) showing the expression of cyclin D2, HA, myc on total lysate of Ctrl, $RACK1_{DE-}$ (DE) and $RACK1_{WT\text{-}his\text{-}myc}$ (WT) cells transfected with the $eIF3d_{HA}$ plasmid. An anti-puromycin antibody was used to measure the puromycin incorporation level. The ponceau (*lower*) shows the protein loading for each line. Bar graphs (*right*) report the band intensity ratio between cyclin D2 to actin, and puromycin to ponceau. Data are mean ± sd. D) qRT-PCR analysis measures the level of cyclin D2 normalized to that of GAPDH mRNA. The bar graph reports the mean ± sd (n = 3 independent experiments).

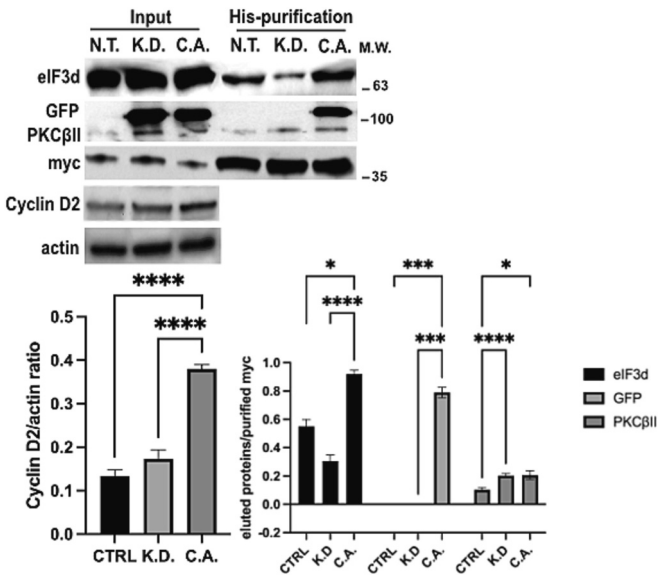

Fig. 3. The ribosomal RACK1/eIF3d binding increases when PKCβII is activated. Representative immunoblotting ($n = 3$ independent experiments) shows the expression of eIF3d, GFP PKCβII and myc on both total lysate and His pull-down eluate in $RACK1_{WT\text{-}his\text{-}myc}$ (WT) expressing either a GFP-tagged catalytically active (C.A.) or inactive (kinase-dead, K.D.) PKCβII. Cyclin D2 and actin immunoblotting in total lysate. Mock (NT) was used as a transfection-negative control. The bar graph (*lower left*) reports the ratio of band intensity between Cyclin D2 and actin and Bar graph (*lower right*) reports the ratio of band intensity between eIF3d, GFP PKCβII to myc. Data are mean ± sd.

assay on heat-shocked MCF-7 and MDA $RACK1_{WT\text{-}his\text{-}myc}$ cells and found similar results (Supplemental Fig. 4A and B).

To understand whether the eIF4E blocking conditions modulate the binding of eIF3d with PIC by ribosomal RACK1, we looked for, among the mRNAs able to bind to eIF3d, those whose translation is induced by heat shock [14]. We found the HSP-70, a mRNA whose translation has been demonstrated to be cap-independent [55–57]. Analysis of the HSP-70 expression by immunoblotting showed that rapamycin administration and heat shock, in addition to increase the RACK1 binding to eIF3d, stimulated more HSP-70 protein than non-treated cells (Fig. 4B). The same results were found for the heat stress-treated MCF-7 and MDA $RACK1_{WT\text{-}his\text{-}myc}$ cells (Supplemental Fig. 3C and D).

As observed for the translation control of cyclin D2 mRNA, we examined the HSP-70 translation when eIF3d is recruited on PIC by $RACK1_{WT\text{-}his\text{-}myc}$. In control cells, the $eIF3d_{HA}$ expression raised the HSP-70 level compared to controls (Fig. 4C). When stably expressing the $RACK1_{WT\text{-}his\text{-}myc}$ cells a larger increase of the HSP-70 protein is observed (Fig. 4C), while the mutant RACK1 does not modify its expression (Fig. 4C). Looking at the HSP-70 expression in $RACK1_{WT\text{-}his\text{-}myc\ cells}$ expressing $eIF3d_{HA}$ we found that HSP-70 expression was more effective than in the case of $eIF3d_{HA}$ alone (Fig. 4C), showing a further increase of expression. Instead, when $eIF3d_{HA}$ is expressed in mutant RACK1 cells the HSP-70 level is like that observed in mutant RACK1 cells, indicating that the RACK1 mutant abolishes their expression stimulated by $eIF3d_{HA}$ (Fig. 4C). These results suggest that HSP-70 translation requires the binding of eIF3d to ribosomal RACK1.

Finally, we also investigated the HSP-70 mRNA expression by qRT-PCR analysis in SH-SY5Y cells expressing $RACK1_{DE\text{-}his\text{-}myc}$ and $RACK1_{WT\text{-}his\text{-}myc}$ and transfected with eIF3d-HA plasmid. The results indicated that the HSP-70 mRNA amounts were unaffected in all investigated cases (Fig. 4D), suggesting that the HSP-70 mRNA expression was modulated at the translational level.

4. Discussion

Numerous studies have shown that ribosomal RACK1 up-regulation leads to an increase in cell proliferation by the eIF4F non-canonical translation [43,58,59]. However, the underlying mechanism has not been fully defined yet. In this work, using the PIC conformational data previously obtained from cryo-EM analyses and the ribosomal RACK1 mutant (R36D/K38E, $RACK1_{DE}$), we demonstrate that up-regulated ribosomal RACK1 recruits eIF3d on 43S PIC for the specific translation of cyclin D2 mRNA. Furthermore, we have found that the active PKCβII promotes the binding of ribosomal RACK1 with eIF3d, suggesting that the RACK1-eIF3d complex might depend on the activation of a specific translational controlling pathway. As support to this suggestion, we find that eIF4F blocking conditions, such as rapamycin administration and heat shock stress, increase the association of ribosomal RACK1 with eIF3d leading to HSP-70 translation.

In previous studies [33,34] and in this study, the $RACK1_{DE\text{-}his\text{-}myc}$ and $RACK1_{WT\text{-}his\text{-}myc}$ have been used to understand the ribosomal RACK1 activity. Supplemental Fig. 1 A reveals a decrease of endogenous RACK1 on ribosomal fractions in $RACK1_{WT\text{-}his\text{-}myc}$ cells which is compensated by the level of $RACK1_{WT\text{-}his\text{-}myc}$ when compared to its endogenous level in $RACK1_{DE\text{-}his\text{-}myc}$ cells. The presence of the two RACK1 forms on the ribosomes, over to confirm the soundness of the HPIPD assay, suggests that RACK1 may form a hetero- and/or homodimer on ribosomes. This is also supported by our HPIPD assay in which a small amount of endogenous RACK1 co-purifies with $RACK1_{WT\text{-}his\text{-}myc}$ (Fig. 1E). The homo- and heterodimerization of RACK1 is required for *N*-methyl-D aspartate receptor [60], thus we cannot exclude that ribosomal RACK1 functions as homo- and heterodimer on the ribosomes However, so far cryo-EM elaborations do not report a RACK1 dimer on ribosomes and, also in this study we observe that endogenous RACK1 co-purifies with RACK1 mutant (Fig. 1E). Thus, further studies are required to determine whether the ribosome own RACK1 dimers and whether they are required to increase the proliferation.

This study shows that RACK1 may act as a ribosomal scaffold for the recruitment of eIF3d on 43S PIC. As inferred from the cryo-EM analyses, RACK1 is located closer to eIF3d, namely behind the head of the 43S and 48S PICs, near to the 5′ exit channel [61]. This position has been thought to be involved in initiation events, such as the binding with eIF3 [62], and in the internal ribosome entry site in viral mRNAs [59]. The RACK1 position is also conserved in the yeast 40s subunit, where, although eIF3d is not expressed, the RACK1/Asc1 interacts with the eIF3c/NIP1 subunit [63]. These findings support our suggestion that ribosomal RACK1 may act as an eIF3d ribosomal scaffold and may contribute to the eIF3d specialized translation, rather than be involved in eIF4F canonical translation. This is supported by the side of the RACK1 on 48S being opposite to the eIF4F complex, reducing its possibility to participate in the eIF4F canonical translation [64,65]. This is in keeping with our HPIPD experiments that confirm the eIF4F and eIF3d positions on 43S/48S PICs. Recent studies have demonstrated that eIF3d controls the translation of specific mRNAs [15] when the eIF4F translation is arrested [12]. This fits in with our findings according to which the inhibition of eIF4F canonical translation by rapamycin and heat shock stress increases the interaction of the ribosomal RACK1 with eIF3d, as we have found. In addition, in this study we report that the eIF3d up-regulation declines the global translation. Although this is in contrast with different reports [66,67], we found that the association of $eIF3d_{HA}$ to PICs by the binding with ribosomal RACK1 leaves out eIF4E leading to decrease of the eIF4E dependent translation, furthermore, supporting our hypothesis.

Our study also shows that the active PKCβII stimulates the interaction of RACK1 with eIF3d. The PKCβII phosphorylation mediated by ribosomal RACK1 on eIFs was described only in the case of eIF6 phosphorylation [48]. Next, it has been found that eIF4E is also phosphorylated by the RACK1-PKCβII complex [41,68]. Furthermore, another eIF3 subunit, eIF3a, is phosphorylated by the RACK1-PKCβII kinase

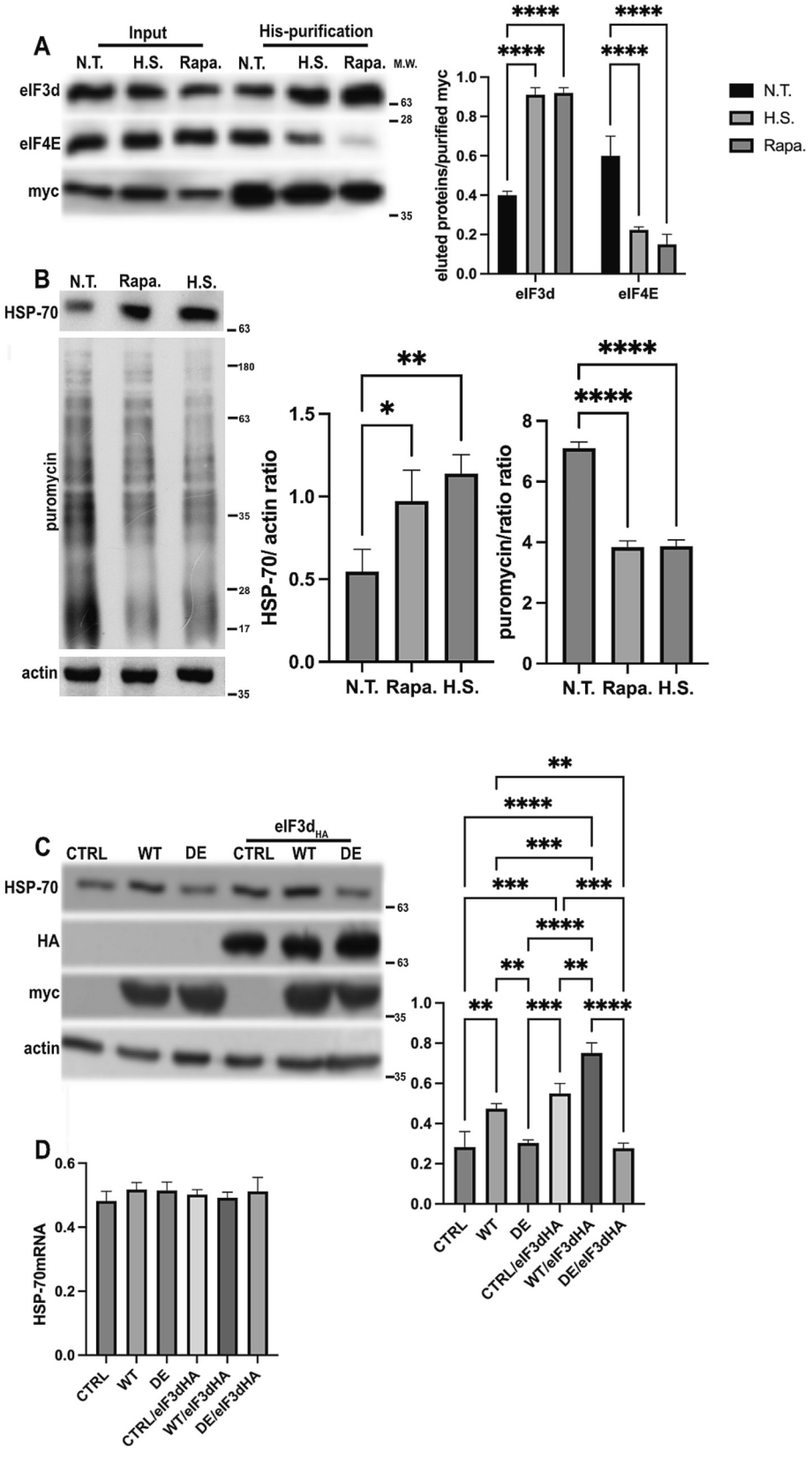

(caption on next page)

Fig. 4. HSP-70 expression induced by MTORC1 inhibiting conditions. A) Representative immunoblotting ($n = 3$ independent experiments) shows the expression of eIF3d, eIF4E and myc on both, total lysate and His pull-down eluate in $RACK1_{WT\text{-}his\text{-}myc}$ (WT) cells treated or not with 500 nM (Rapa) or 44 °C for 30 min. The bar graph (*right*) reports the ratio of band intensity between eIF3d and eIF4E to Myc in His purification assay. Data are mean ± sd. B) Representative immunoblotting (n = 3 independent experiments) shows the expression of HSP-70, puromycin incorporation and actin on total lysate of $RACK1_{WT\text{-}his\text{-}myc}$ (WT) cells treated or not with 500 nM (Rapa) or 44 °C for 30 min. The bar graph (*right*) reports the band intensity ratio between HSP-70, Puromycin and actin. Data are mean ± sd. C) representative immunoblotting (n = 3 independent experiments) shows the expression of HSP-70, HA, myc and actin on total lysate of Ctrl, $RACK1_{DE\text{-}}$ (DE) and $RACK1_{WT\text{-}his\text{-}myc}$ (WT) cells transfected with the $eIF3d_{HA}$ plasmid. Bar graph (*right*) reports the band intensity ratio between HSP-70 and actin. Data are mean ± sd. D) qRT-PCR analysis to measure the level of HSP-70 mRNA normalized to those of GAPDH mRNA. The bar graph reports the mean ± sd (n = 3 independent experiments).

complex [40]. Interestingly, eIF3a is positioned on the 43S PIC near RACK1 but in the site opposite to eIF3d. Such a position of eIF3a does not exclude the possibility for PKCβII kinase to bind and, eventually, phosphorylate both eIF3 subunits [19] and demonstrates that RACK1 is not an exclusive ribosomal scaffold for the eIF3d but also other eIF3 subunits. Nevertheless, further studies are needed to demonstrate that active PKCβII can phosphorylate eIF3d to modulate its activity. In this context, it is useful to remind, that eIF3d is phosphorylated by the Casein I kinase [12].

We have shown that the binding of ribosomal RACK1 to the eIF3d-RACK1 complex is also induced by heat shock stress, which is known to block translational initiation [69]. It has been reported that glucose deprivation, a nutrient stress, promotes the activation of eIF3d specialized translation [12]. Furthermore, the persistent integrated stress response is controlled by eIF3d specialized translation [53], supporting the critical role of eIF3d under stress conditions. RACK1 plays a role in ribosome-associated quality control (RQC), in which stress signaling promote the dissociation of stalled ribosomes in the elongation phase and the recycling of 40S subunits in a new round of translation [70,71]. Although heat shock is a stress factor different from glucose deprivation, our results suggest that the increased interaction of RACK1 and eIF3d under stress conditions may lead to fast recycling of 40S subunit for a new round of translation.

Finally, we found that when ribosomal RACK1 is driven to associate with eIF3d, as in the case of $eIF3d_{HA}$ expression, rapamycin administration or heat shock, the HSP-70 protein expression increases. The HPS-70 mRNA is known to be transcriptionally and cap-independent translationally regulated following a heat shock mediated by N6-methyladenosine (m^6A) in 5'UTR [55–57]. In turn, The eIF3 complex uses 5'UTR (m^6A) to promote the cap-independent translation, and eIF3d is, among the eIF3 subunits, a candidate for binding to m^6A [55]. HPS-70 mRNA has been also purified by eIF3d pull-down [14]. In yeast, the Asc1/RACK1 binds and controls the translation of the SSA4, the most heat stress-inducible HSP-70 mRNA family [72]. Therefore, the present and the previous findings suggest that the formation of the ribosomal RACK1-eIF3d complex is mainly driven by the change of the translational conditions as in the case of the translation of specific mRNAs. However, additional experiments are needed to ascertain this idea.

5. Conclusions

This study establishes that the scaffold ribosomal RACK1 binds eIF3d on ribosomes to control the specialized translation in eIF4F independent manner, and to modulate eIF3d function by PKCβII kinase. In this context, the PKCβII kinase-eIF3d-RACK1 axis may represent a new mechanism of translational control alternative to mTORC1 pathway.

Supplementary data to this article can be found online at https://doi.org/10.1016/j.cellsig.2024.111494.

Author contributions

FS and RM performed and analyzed experiments, EC, DC and NR provided data analysis and discussion, FT and DW provided data analysis and discussion, SR wrote the manuscript, MC conceived and analyzed experiments and wrote the manuscript.

Funding

Please add: "This work was supported by grants from the Italian Ministry of Education, University and Research: "PRIN2017" to D.C.; "Departments of Excellence-2018" Program (Dipartimenti di Eccellenza) to DIBAF (University of Tuscia, Viterbo, Italy) (Project "Landscape 4.0 - food, wellbeing and environment") to D.C. The funders had no role in study design, data collection and analysis, decision to publish or preparation of the manuscript.

CRediT authorship contribution statement

Federica Silvestri: Formal analysis, Conceptualization. **Raffaele Montuoro:** Methodology, Formal analysis, Conceptualization. **Elisabetta Catalani:** Methodology. **Francesca Tilesi:** Methodology. **Daniela Willems:** Methodology. **Nicla Romano:** Supervision. **Sara Ricciardi:** Data curation. **Davide Cervia:** Supervision. **Marcello Ceci:** Writing – original draft, Conceptualization.

Declaration of competing interest

None.

Data availability

Data will be made available on request.

Acknowledgments

We thank members of the Ceci Lab for useful discussion, prof. Jamie Cate (University of California, Berkley) for the eIF3dHA plasmids, the prof. Alexandra Newton (University of California at San Diego) for GFP-PKCβII plasmids.

References

[1] P. Calamita, G. Gatti, A. Miluzio, A. Scagliola, S. Biffo, Translating the game: ribosomes as active players, Front. Genet. 9 (2018) 533.
[2] M.L. Truitt, D. Ruggero, New frontiers in translational control of the cancer genome, Nat. Rev. Cancer 16 (5) (2016) 288–304.
[3] A.G. Hinnebusch, I.P. Ivanov, N. Sonenberg, Translational control by 5′-untranslated regions of eukaryotic mRNAs, Science 352 (6292) (2016) 1413–1416.
[4] S. Gallo, N. Manfrini, Working hard at the nexus between cell signaling and the ribosomal machinery: an insight into the roles of RACK1 in translational regulation, Translation (Austin) 3 (2) (2015) e1120382.
[5] J. Pelletier, T.M. Schmeing, N. Sonenberg, The multifaceted eukaryotic cap structure, Wiley Interdiscip Rev RNA 12 (2) (2021) e1636.
[6] R. Cencic, J. Pelletier, A cautionary note on the use of cap analogue affinity resins, Anal. Biochem. 560 (2018) 24–29.
[7] B. Kim, J. Seol, Y.K. Kim, J.B. Lee, Single-molecule visualization of mRNA circularization during translation, Exp. Mol. Med. 55 (2) (2023) 283–289.
[8] J.L. Banko, F. Poulin, L. Hou, C.T. DeMaria, N. Sonenberg, E. Klann, The translation repressor 4E-BP2 is critical for eIF4F complex formation, synaptic plasticity, and memory in the hippocampus, J. Neurosci. 25 (42) (2005) 9581–9590.
[9] A.C. Gingras, N. Sonenberg, Adenovirus infection inactivates the translational inhibitors 4E-BP1 and 4E-BP2, Virology 237 (1) (1997) 182–186.
[10] D. Simsek, G.C. Tiu, R.A. Flynn, G.W. Byeon, K. Leppek, A.F. Xu, H.Y. Chang, M. Barna, The mammalian Ribo-interactome reveals ribosome functional diversity and heterogeneity, Cell 169 (6) (2017) 1051–1065.e18.
[11] R. Nicastro, L. Brohee, J. Alba, J. Nuchel, G. Figlia, S. Kipschull, P. Gollwitzer, J. Romero-Pozuelo, S.A. Fernandes, A. Lamprakis, S. Vanni, A.A. Teleman, C. De Virgilio, C. Demetriades, Malonyl-CoA is a conserved endogenous ATP-competitive mTORC1 inhibitor, Nat. Cell Biol. 25 (9) (2023) 1303–1318.

[12] A.M. Lamper, R.H. Fleming, K.M. Ladd, A.S.Y. Lee, A phosphorylation-regulated eIF3d translation switch mediates cellular adaptation to metabolic stress, Science 370 (6518) (2020) 853–856.
[13] M.D. Smith, L. Arake-Tacca, A. Nitido, E. Montabana, A. Park, J.H. Cate, Assembly of eIF3 mediated by mutually dependent subunit insertion, Structure 24 (6) (2016) 886–896.
[14] A.S. Lee, P.J. Kranzusch, J.H. Cate, eIF3 targets cell-proliferation messenger RNAs for translational activation or repression, Nature 522 (7554) (2015) 111–114.
[15] A.S. Lee, P.J. Kranzusch, J.A. Doudna, J.H. Cate, eIF3d is an mRNA cap-binding protein that is required for specialized translation initiation, Nature 536 (7614) (2016) 96–99.
[16] C. de la Parra, A. Ernlund, A. Alard, K. Ruggles, B. Ueberheide, R.J. Schneider, A widespread alternate form of cap-dependent mRNA translation initiation, Nat. Commun. 9 (1) (2018) 3068.
[17] V. Volta, S. Perez-Baos, C. de la Parra, O. Katsara, A. Ernlund, S. Dornbaum, R. J. Schneider, A DAP5/eIF3d alternate mRNA translation mechanism promotes differentiation and immune suppression by human regulatory T cells, Nat. Commun. 12 (1) (2021) 6979.
[18] A.G. Hinnebusch, eIF3: a versatile scaffold for translation initiation complexes, Trends Biochem. Sci. 31 (10) (2006) 553–562.
[19] A. Des Georges, V. Dhote, L. Kuhn, C.U. Hellen, T.V. Pestova, J. Frank, Y. Hashem, Structure of mammalian eIF3 in the context of the 43S preinitiation complex, Nature 525 (7570) (2015) 491–495.
[20] J.P. Erzberger, F. Stengel, R. Pellarin, S. Zhang, T. Schaefer, C.H.S. Aylett, P. Cimermancic, D. Boehringer, A. Sali, R. Aebersold, N. Ban, Molecular architecture of the 40S·eIF1·eIF3 translation initiation complex, Cell 159 (5) (2014) 1227–1228.
[21] C.H. Aylett, D. Boehringer, J.P. Erzberger, T. Schaefer, N. Ban, Structure of a yeast 40S-eIF1-eIF1A-eIF3-eIF3j initiation complex, Nat. Struct. Mol. Biol. 22 (3) (2015) 269–271.
[22] Y. Hashem, A. Des Georges, V. Dhote, R. Langlois, H.Y. Liao, R.A. Grassucci, C. U. Hellen, T.V. Pestova, J. Frank, Structure of the mammalian ribosomal 43S preinitiation complex bound to the scanning factor DHX29, Cell 153 (5) (2013) 1108–1119.
[23] T. Hussain, J.L. Llacer, I.S. Fernandez, A. Munoz, P. Martin-Marcos, C.G. Savva, J. R. Lorsch, A.G. Hinnebusch, V. Ramakrishnan, Structural changes enable start codon recognition by the eukaryotic translation initiation complex, Cell 159 (3) (2014) 597–607.
[24] M.H. Nielsen, R.K. Flygaard, L.B. Jenner, Structural analysis of ribosomal RACK1 and its role in translational control, Cell. Signal. 35 (2017) 272–281.
[25] D. Ron, C.H. Chen, J. Caldwell, L. Jamieson, E. Orr, D. Mochly-Rosen, Cloning of an intracellular receptor for protein kinase C: a homolog of the beta subunit of G proteins, Proc. Natl. Acad. Sci. USA 91 (3) (1994) 839–843.
[26] S. Dwane, E. Durack, R. O'Connor, P.A. Kiely, RACK1 promotes neurite outgrowth by scaffolding AGAP2 to FAK, Cell. Signal. 26 (1) (2014) 9–18.
[27] M. Kiely, D.R. Adams, S.L. Hayes, R. O'Connor, G.S. Baillie, P.A. Kiely, RACK1 stabilises the activity of PP2A to regulate the transformed phenotype in mammary epithelial cells, Cell. Signal. 35 (2017) 290–300.
[28] G.B. Bolger, The RNA-binding protein SERBP1 interacts selectively with the signaling protein RACK1, Cell. Signal. 35 (2017) 256–263.
[29] S.J. Yarwood, E. Parnell, R.J. Bird, The cyclic AMP phosphodiesterase 4D5 (PDE4D5)/receptor for activated C-kinase 1 (RACK1) signalling complex as a sensor of the extracellular nano-environment, Cell. Signal. 35 (2017) 282–289.
[30] D. Duff, A. Long, Roles for RACK1 in cancer cell migration and invasion, Cell. Signal. 35 (2017) 250–255.
[31] L. Kershner, K. Welshhans, RACK1 regulates neural development, Neural Regen. Res. 12 (7) (2017) 1036–1039.
[32] H.D. Kim, E. Kong, Y. Kim, J.S. Chang, J. Kim, RACK1 depletion in the ribosome induces selective translation for non-canonical autophagy, Cell Death Dis. 8 (5) (2017) e2800.
[33] N. Romano, B. Di Giacomo, V. Nobile, A. Borreca, D. Willems, F. Tilesi, E. Catalani, M. Agrawal, K. Welshhans, S. Ricciardi, D. Cervia, M. Ceci, Ribosomal RACK1 regulates the dendritic Arborization by repressing FMRP activity, Int. J. Mol. Sci. 23 (19) (2022).
[34] N. Romano, M. Veronese, N. Manfrini, L. Zolla, M. Ceci, Ribosomal RACK1 promotes proliferation of neuroblastoma cells independently of global translation upregulation, Cell. Signal. 53 (2019) 102–110.
[35] T.R. Baffi, A.N. Van, W. Zhao, G.B. Mills, A.C. Newton, Protein kinase C quality control by phosphatase PHLPP1 unveils loss-of-function mechanism in cancer, Mol. Cell 74 (2) (2019) 378–392 e5.
[36] A. Russo, R. Scardigli, F. La Regina, M.E. Murray, N. Romano, D.W. Dickson, B. Wolozin, A. Cattaneo, M. Ceci, Increased cytoplasmic TDP-43 reduces global protein synthesis by interacting with RACK1 on polyribosomes, Hum. Mol. Genet. 26 (8) (2017) 1407–1418.
[37] M. Ceci, K. Welshhans, M.T. Ciotti, R. Brandi, C. Parisi, F. Paoletti, L. Pistillo, G. J. Bassell, A. Cattaneo, RACK1 is a ribosome scaffold protein for β-actin mRNA/ZBP1 complex, PLoS One 7 (4) (2012) e35034.
[38] H. Sun, J. Shang, X. Liu, S. Ren, S. Hu, X. Wang, Eukaryotic initiation factor 3a promotes the development of diffuse large B-cell lymphoma through regulating cell proliferation, BMC Cancer 24 (1) (2024) 432.
[39] A. Alard, O. Katsara, T. Rios-Fuller, C. Parra, U. Ozerdem, A. Ernlund, R. J. Schneider, Breast cancer cell mesenchymal transition and metastasis directed by DAP5/eIF3d-mediated selective mRNA translation, Cell Rep. 42 (6) (2023) 112646.
[40] M.I. Dobrikov, E.Y. Dobrikova, M. Gromeier, Ribosomal RACK1: Protein Kinase C βII phosphorylates eukaryotic initiation factor 4G1 at S1093 to modulate cap-dependent and -independent translation initiation, Mol. Cell. Biol. 38 (19) (2018).
[41] M.I. Dobrikov, E.Y. Dobrikova, M. Gromeier, Ribosomal RACK1:Protein Kinase C βII modulates intramolecular interactions between unstructured regions of eukaryotic initiation factor 4G (eIF4G) that control eIF4E and eIF3 binding, Mol. Cell. Biol. 38 (19) (2018).
[42] S.M. Coyle, W.V. Gilbert, J.A. Doudna, Direct link between RACK1 function and localization at the ribosome in vivo, Mol. Cell. Biol. 29 (6) (2009) 1626–1634.
[43] Y. Ruan, L. Sun, Y. Hao, L. Wang, J. Xu, W. Zhang, J. Xie, L. Guo, L. Zhou, X. Yun, H. Zhu, A. Shen, J. Gu, Ribosomal RACK1 promotes chemoresistance and growth in human hepatocellular carcinoma, J. Clin. Invest. 122 (7) (2012) 2554–2566.
[44] M.K. Thompson, M.F. Rojas-Duran, P. Gangaramani, W.V. Gilbert, The ribosomal protein Asc1/RACK1 is required for efficient translation of short mRNAs, Elife 5 (2016).
[45] F. Zhang, S. Xiang, Y. Cao, M. Li, Q. Ma, H. Liang, H. Li, Y. Ye, Y. Zhang, L. Jiang, Y. Hu, J. Zhou, X. Wang, L. Nie, X. Liang, W. Gong, Y. Liu, EIF3D promotes gallbladder cancer development by stabilizing GRK2 kinase and activating PI3K-AKT signaling pathway, Cell Death Dis. 8 (6) (2017) e2868.
[46] H. Li, F. Zhou, H. Wang, D. Lin, G. Chen, X. Zuo, L. Sun, X. Zhang, S. Yang, Knockdown of EIF3D suppresses proliferation of human melanoma cells through G2/M phase arrest, Biotechnol. Appl. Biochem. 62 (5) (2015) 615–620.
[47] D. Mochly-Rosen, B.L. Smith, C.H. Chen, M.H. Disatnik, D. Ron, Interaction of protein kinase C with RACK1, a receptor for activated C-kinase: a role in beta protein kinase C mediated signal transduction, Biochem. Soc. Trans. 23 (3) (1995) 596–600.
[48] M. Ceci, C. Gaviraghi, C. Gorrini, L.A. Sala, N. Offenhäuser, P.C. Marchisio, S. Biffo, Release of eIF6 (p27BBP) from the 60S subunit allows 80S ribosome assembly, Nature 426 (6966) (2003) 579–584.
[49] V. Parrow, E. Nanberg, J. Heikkila, U. Hammerling, S. Pahlman, Protein kinase C remains functionally active during TPA induced neuronal differentiation of SH-SY5Y human neuroblastoma cells, J. Cell. Physiol. 152 (3) (1992) 536–544.
[50] U. Trollér, R. Zeidman, K. Svensson, C. Larsson, A PKCbeta isoform mediates phorbol ester-induced activation of Erk1/2 and expression of neuronal differentiation genes in neuroblastoma cells, FEBS Lett. 508 (1) (2001) 126–130.
[51] P. LoPresti, W. Poluha, D.K. Poluha, E. Drinkwater, A.H. Ross, Neuronal differentiation triggered by blocking cell proliferation, Cell Growth Different. Mol. Biol. J. Am. Assoc. Cancer Res. 3 (9) (1992) 627–635.
[52] S. Capsoni, S. Covaceuszach, S. Marinelli, M. Ceci, A. Bernardo, L. Minghetti, G. Ugolini, F. Pavone, A. Cattaneo, Taking pain out of NGF: a "painless" NGF mutant, linked to hereditary sensory autonomic neuropathy type V, with full neurotrophic activity, PLoS One 6 (2) (2011) e17321.
[53] S. Mukhopadhyay, M.E. Amodeo, A.S.Y. Lee, eIF3d controls the persistent integrated stress response, Mol. Cell 83 (18) (2023) 3303–3313, e6.
[54] M.E. Hester, M.J. Murtha, S. Song, M. Rao, C.J. Miranda, K. Meyer, J. Tian, G. Boulting, D.V. Schaffer, M.X. Zhu, S.L. Pfaff, F.H. Gage, B.K. Kaspar, Rapid and efficient generation of functional motor neurons from human pluripotent stem cells using gene delivered transcription factor codes, Mol. Ther. 19 (10) (2011) 1905–1912.
[55] K.D. Meyer, D.P. Patil, J. Zhou, A. Zinoviev, M.A. Skabkin, O. Elemento, T. V. Pestova, S.B. Qian, S.R. Jaffrey, 5' UTR m(6)A promotes cap-independent translation, Cell 163 (4) (2015) 999–1010.
[56] S. Lindquist, E.A. Craig, The heat-shock proteins, Annu. Rev. Genet. 22 (1988) 631–677.
[57] J. Zhou, J. Wan, X. Gao, X. Zhang, S.R. Jaffrey, S.B. Qian, Dynamic m(6)A mRNA methylation directs translational control of heat shock response, Nature 526 (7574) (2015) 591–594.
[58] V. Volta, A. Beugnet, S. Gallo, L. Magri, D. Brina, E. Pesce, P. Calamita, F. Sanvito, S. Biffo, RACK1 depletion in a mouse model causes lethality, pigmentation deficits and reduction in protein synthesis efficiency, Cell. Mol. Life Sci. 70 (8) (2013) 1439–1450.
[59] K. Majzoub, M.L. Hafirassou, C. Meignin, A. Goto, S. Marzi, A. Fedorova, Y. Verdier, J. Vinh, J.A. Hoffmann, F. Martin, T.F. Baumert, C. Schuster, J.L. Imler, RACK1 controls IRES-mediated translation of viruses, Cell 159 (5) (2014) 1086–1095.
[60] C. Thornton, K.C. Tang, K. Phamluong, K. Luong, A. Vagts, D. Nikanjam, R. Yaka, D. Ron, Spatial and temporal regulation of RACK1 function and N-methyl-D-aspartate receptor activity through WD40 motif-mediated dimerization, J. Biol. Chem. 279 (30) (2004) 31357–31364.
[61] A. Herrmannova, T. Prilepskaja, S. Wagner, D. Sikrova, J. Zeman, K. Poncova, L. S. Valasek, Adapted formaldehyde gradient cross-linking protocol implicates human eIF3d and eIF3c, k and l subunits in the 43S and 48S pre-initiation complex assembly, respectively, Nucleic Acids Res. 48 (4) (2020) 1969–1984.
[62] K. Schmitt, N. Smolinski, P. Neumann, S. Schmaul, V. Hofer-Pretz, G.H. Braus, O. Valerius, Asc1p/RACK1 connects ribosomes to eukaryotic Phosphosignaling, Mol. Cell. Biol. 37 (3) (2017).
[63] T. Kouba, E. Rutkai, M. Karásková, L. Valášek, The eIF3c/NIP1 PCI domain interacts with RNA and RACK1/ASC1 and promotes assembly of translation preinitiation complexes, Nucleic Acids Res. 40 (6) (2012) 2683–2699.
[64] J. Brito Querido, M. Sokabe, S. Kraatz, Y. Gordiyenko, J.M. Skehel, C.S. Fraser, V. Ramakrishnan, Structure of a human 48S translational initiation complex, Science 369 (6508) (2020) 1220–1227.
[65] L. Yatime, K.L. Hein, J. Nilsson, P. Nissen, Structure of the RACK1 dimer from *Saccharomyces cerevisiae*, J. Mol. Biol. 411 (2) (2011) 486–498.
[66] S. Wagner, A. Herrmannova, D. Sikrova, L.S. Valasek, Human eIF3b and eIF3a serve as the nucleation core for the assembly of eIF3 into two interconnected

modules: the yeast-like core and the octamer, Nucleic Acids Res. 44 (22) (2016) 10772–10788.
[67] M. Shah, D. Su, J.S. Scheliga, T. Pluskal, S. Boronat, K. Motamedchaboki, A. R. Campos, F. Qi, E. Hidalgo, M. Yanagida, D.A. Wolf, A transcript-specific eIF3 complex mediates global translational control of energy metabolism, Cell Rep. 16 (7) (2016) 1891–1902.
[68] S. Gallo, S. Ricciardi, N. Manfrini, E. Pesce, S. Oliveto, P. Calamita, M. Mancino, E. Maffioli, M. Moro, M. Crosti, V. Berno, M. Bombaci, G. Tedeschi, S. Biffo, RACK1 specifically regulates translation through its binding to ribosomes, Mol. Cell. Biol. 38 (23) (2018).
[69] S. Ma, R.B. Bhattacharjee, J. Bag, Expression of poly(A)-binding protein is upregulated during recovery from heat shock in HeLa cells, FEBS J. 276 (2) (2009) 552–570.
[70] E. Sundaramoorthy, M. Leonard, R. Mak, J. Liao, A. Fulzele, E.J. Bennett, ZNF598 and RACK1 regulate mammalian ribosome-associated quality control function by mediating regulatory 40S ribosomal Ubiquitylation, Mol. Cell 65 (4) (2017) 751–760.e4.
[71] M.G. Rollins, M. Shasmal, N. Meade, H. Astar, P.S. Shen, D. Walsh, Negative charge in the RACK1 loop broadens the translational capacity of the human ribosome, Cell Rep. 36 (10) (2021) 109663.
[72] L.R. Alagar Boopathy, E. Beadle, A.R. Xiao, A. Garcia-Bueno Rico, C. Alecki, I. Garcia De Andres, K. Edelmeier, L. Lazzari, M. Amiri, M. Vera, The ribosome quality control factor Asc1 determines the fate of HSP70 mRNA on and off the ribosome, Nucleic Acids Res. 51 (12) (2023) 6370–6388.